Large-eddy simulation of scaled floating wind turbines in a boundary layer wind tunnel

IOP Conf. Series: Journal of Physics: Conf. Series **1037** (2018) 072032 doi:10.1088/1742-6596/1037/7/072032

Large-eddy simulation of scaled floating wind turbines in a boundary layer wind tunnel

J Wang[1], C Wang[1], O D Castañeda[1], F Campagnolo[1], C L Bottasso[1,2]

[1] Wind Energy Institute, Technische Universität München, Boltzmannstraße 15, D-85748 Garching bei München, Germany

[2] Dipartimento di Scienze e Tecnologie Aerospaziali, Politecnico di Milano, Via La Masa 34, I-20156 Milano, Italy

E-mail: jesse.wang@tum.de

Abstract. Floating offshore wind turbines are attracting an ever increasing interest for deep-water applications. Among the many different research aspects of floating offshore technology, understanding wake interactions of multiple floating wind turbines under complex motions is a particularly challenging task, which requires both suitable high-fidelity numerical models and relevant experimental observations. In this work, we first present a framework for the large-eddy simulation of FOWTs. Then, the simulation model is verified with the help of wind tunnel experimental data. Measurements were obtained in a neutrally stratified atmospheric boundary layer for very closely spaced wind turbine models, whose pitching motion is prescribed to simulate various wave-wind conditions. The pitching motion of the wind turbines induces vertical meandering of the wakes that interact with downstream turbines. Simulations are compared to experimental measurements in terms of inflow conditions and turbine response parameters, showing a reasonable matching, although longer runs are necessary for a more complete characterization of the results.

1. Introduction

Floating offshore wind turbine (FOWT) technology currently represents one of the most significant engineering challenges in the wind energy field. The technology is now moving towards deeper waters, where the wind resource is exceptionally abundant. In this regard, single and multi-turbine floating platforms are now being actively investigated.

A wind tunnel experimental campaign [6] was recently conducted using a scaled model of a floating platform concept, developed by the Korea Research Institute of Ships & Ocean Engineering (KRISO) [12]. The square-shaped platform is equipped with four very closely spaced wind turbines located at its corners. A distinguishing characteristic of this and similar systems is that there is not only a complex interaction between the atmospheric flow and the wind turbines, but also among the wind turbines themselves. Indeed, wakes shed by the upwind wind turbines affect power and loads of downstream machines. In this sense, wakes represent a major form of coupling within the power plant. In addition, the platform dynamics will affect the wind turbine response, modifying performance and loads.

This paper presents a large-eddy simulation (LES) of that experiment, and performs a first step towards the validation of the numerical framework by using experimental data. It is expected that a validated numerical model could be successfully used to simulate full-scale

multiple-turbine floating platforms, and thus provide valuable insight into the combined effects of wakes and platform motion on the performance and loading of FOWTs.

2. Numerical model

2.1. LES framework

The LES framework is developed within `SOWFA` [7], a code based on a standard incompressible formulation in the OpenFOAM repository. The code, which represents the rotor by an actuator line method interacting with the LES model, is coupled with the structural dynamic model implemented in `FAST` [9]. An immersed boundary formulation is used to model the wind turbine nacelle, tower and the floating platform [16]. A customized Scotch parallelized decomposition method (see §4) is used to improve the computational efficiency of the numerical procedures. In the simulation environment, the wind turbine models are operated by the same pitch and torque controller used in the experiments. Wang et al. [14, 16] have presented the validation of the present computational framework for single/multiple bottom-fixed scaled wind turbine models.

All spatially discretized terms in the governing equations are obtained by centered differencing, except for the convection term. Indeed, a deferred correction Gamma-bounded interpolation method [8] is used for the convection term, which allows one to control the level of upwinding. Temporal discretization is based on a second-order backward Euler scheme. The symmetric matrices associated with pressure are solved by a conjugate gradient algorithm, while non-symmetric matrices associated with velocity and temperature by a bi-conjugate gradient solver. The PISO time stepping algorithm is used to recursively correct the pressure flux equation.

2.2. Floating algorithm

2.2.1. Coordinate transformation The code is modified to accommodate a generic three-dimensional motion of the wind turbines within the computational domain, as caused by the motion of the floating platform. In order to mimic the experiments, the simulated motion of the platform is prescribed by a suitable time history, as discussed later in §2.2.3.

To simplify the implementation, the `FAST` model is not actually moved within the CFD domain, but the relevant coupling quantities are transformed according to the rigid body motion induced by the platform. It should be noticed that this approach is limited to a rigid wind turbine model, and it would not be applicable to a flexible one. Following this procedure, the components $\mathbf{x}_s$ of the position vector of a point in the structural model frame (subscript $(\cdot)_s$) are transformed into the components $\mathbf{x}_f$ in the fluid model reference frame (subscript $(\cdot)_f$) as $\mathbf{x}_s = \mathbf{R}\mathbf{x}_f$, where $\mathbf{R}(t)$ is the time-dependent direction cosine rotation matrix associated with the given prescribed motion. Accordingly, the velocity vector components in the two frames are readily obtained as

$$\dot{\mathbf{x}}_s = \omega \times (\mathbf{R}\mathbf{x}_f) + \mathbf{R}\dot{\mathbf{x}}_f, \tag{1}$$

where $\omega(t)$ indicates the components of the angular velocity vector, and $\dot{(\cdot)}$ indicates a derivative with respect to time t. Therefore, given the velocity at a point on the CFD domain, the velocity seen by the lifting line on the `FAST` model can be readily computed. Once the corresponding aerodynamic force $\mathbf{f}_s$ at that lifting line station has been computed based on the stored lift and drag look up tables, that same force can be mapped back to the CFD frame by the inverse transformation, i.e. $\mathbf{f}_f = \mathbf{R}^T\mathbf{f}_s$.

The immersed boundary subroutine applies a similar transformation in order to account for motion-induced effects. This way, only the boundary conditions and corresponding forces change because of the body motion, while the grid does not. The computational cost is therefore drastically reduced.

This procedure reconstructs the velocity at the lifting line and boundary surfaces, but clearly not the accelerations. Therefore, its use is limited to a rigid model and to cases where one is not interested in the complete loading of the structure, but only on the resulting aerodynamic forces. However, this is indeed the scope of the present work, and the use of this approach results in a much reduced computational cost than in the case of a more rigorous fluid-structure interaction formulation.

2.2.2. Restart capability The code implements a complete restart capability for all its coupled components, including CFD solver, structural dynamic model, immersed boundary formulation and wind turbine controllers. This is of great practical utility given the large computational cost of these simulations, as it allows for consecutive shorter runs. The ability to restart a simulation is obtained by saving to files all necessary internal information, so that a seamless solution is obtained, identical to the one that would have been computed without restarting. While `FAST` already allows for restarts, other components of the code had to be modified. The OpenFOAM immersed boundary subroutine reads a CAD file and uses geometric information to identify the boundary surface in the CFD domain for each time step [10]. If the geometry moves, the solver computes the associated displacement and creates a new CAD file, which therefore needs to be saved and read back for the restart run.

2.2.3. Prescribed platform motion Preliminary estimates provided by KRISO show that, for the specific configuration considered here, the dynamic effects of the wind turbines on the platform motion are negligible. This is because the ratio between platform and wind turbine inertia is significantly larger than the one of other semi-submersible systems. It is therefore expected that the floating platform dynamics will primarily be affected by forces induced by currents, waves and moorings lines [13]. In such a case, a simple one-way coupling exists between the floating platform and the wind turbines dynamics. In this regard, only the platform pitch rotation was prescribed in the experimental setup. In fact, of the six rigid body degrees of freedom of the platform, the pitching motion is the one that is expected to have the larger impact on the wind turbine aerodynamics.

A periodic pitch motion was prescribed to simplify the experimental implementation and to account for limitations of the hardware. The prescribed motion is not scaled as the rest of the model, and results in a higher amplitude and smaller ratio frequency/rotor-speed than the full-scale system. Despite the prescribed platform motion not being properly scaled, the motion-induced wind speed changes with respect to the free stream at hub height are indeed correctly scaled. This ensures that the effects produced by the platform pitch motion on the turbine aerodynamics are properly captured.

2.3. Multi-airfoil polar identification

As mentioned earlier on, an actuator line method is used to represent the interaction of the wind turbine blades with the flow. To this aim, it is necessary to provide, for every airfoil along the blade, the lift and drag coefficients (C_L and C_D, respectively) as functions of the angle of attack and Reynolds number. Since the resulting aerodynamic forces become forcing terms on the flow domain, the accuracy of these coefficients directly affects the quality of the results.

In order to enhance their accuracy, a system identification procedure is used to tune the lift and drag coefficients by means of wind tunnel measurements of rotor thrust and torque [2].

The given nominal values of either lift or drag are corrected with an additional term:

$$C_k(\alpha, \eta, Re) = C_k^0(\alpha, \eta, Re) + \Delta_k(\alpha, \eta, Re), \tag{2}$$

where $C_k^0(k = L$ for lift or $k = D$ for drag) is the nominal value, while $\Delta_k(\alpha, \eta, Re)$ is the unknown correction. This latter term can be expressed as a linear combination of assumed

shape functions:

$$\Delta_k(\alpha, \eta, Re) = \mathbf{n}^T(\alpha, \eta, Re)\mathbf{p}_k, \tag{3}$$

where $\mathbf{p}_k$ is the vector of unknown nodal values and $\mathbf{n}(\alpha, \eta, Re)$ is the vector of shape functions that linearly interpolate along the blade non-dimensional span η and the airfoil Reynolds Re. The shape functions are determined through the singular value decomposition of the Fisher information matrix of the system [2]. To determine the optimal values for $\mathbf{p}_k$, the gradient-based optimization algorithm implemented in the *fmincon* function of `MATLAB` is employed. This function minimizes the cost function:

$$J = \mathbf{e}^T\mathbf{e}, \tag{4}$$

where $\mathbf{e}$ is the discrepancy of power and thrust coefficients between `WT-Perf` predictions and experimental measurements. To identify the polars, 158 operating conditions were tested at different tip-speed-ratios (TSR), blade pitch angles and rotational speeds, covering a range of angles of attack between -3 deg and 10 deg and Reynolds numbers between 10000 and 90000.

3. Experimental setup

Experiments were conducted in a 36 m $\times$ 16.7 m $\times$ 3.84 m boundary layer wind tunnel at Politecnico di Milano [18]. Figure 1 shows the scaled platform model equipped with four wind turbines in the wind tunnel. Two electric motors are located on the floor, orthogonally to the stream-wise flow direction, and are used to vary the platform pitch attitude. Two slender bars aligned with the streamwise flow direction are connected to the two motors, each bar carrying two wind turbines. Although there is no mechanical connection between the two bars, the two motors are operated in order to realize the same motion of the two turbine pairs.

The spires visible at the tunnel inlet (left image in Fig. 1) are turbulence generators [18], which induce a sheared turbulent inflow of desired characteristics. For this particular experiment, the turbulence intensity measured 3D upstream of the platform is roughly equal to 6%, while the wind speed is approximatively equal to 6 m/s. At this wind speed, the G1 turbines operate in the full power region III.

Figure 1: Floating offshore wind turbine scaled model in the boundary layer wind tunnel. Left: view looking upstream towards the tunnel inlet; right: lateral view.

3.1. Wind turbine model

Tests were performed with four scaled G1 wind turbine models, whose rotor diameter and rated rotor speed are equal to 1.1 m and 850 RPM, respectively. The models, already used for other research projects [3–5], are characterized by a realistic aerodynamic performance, notwithstanding the low Reynolds at which the airfoils operate. The rotor wake is characterized by a shape, deficit, and recovery that is in good accordance with those of full-scale machines. The

models feature active collective pitch and torque control that, together with a comprehensive onboard sensorization of the machine (including measures of shaft and tower loads), enables the testing of modern turbine and farm-level control strategies.

3.2. Wind turbine controller

The G1 pitch and torque are managed by a closed-loop controller, implemented on a M1 Bachmann hard-real-time module. The controllers reacts to the turbulent inflow variations, as well as to the periodic relative-speed changes produced by the floating platform oscillations. The controller computes the desired blade pitch β_B and torque demands, which are in turn sent to the actuator control boards. All wind turbine models use the same control algorithm that targets two main functions: power control and load reduction.

4. Computational setup

The two plots in Fig. 2 show a cross-section of the computational domain. The simulation strictly adheres to the experiment, including the domain size and position of the floating platform. The platform is located in the middle of the wind tunnel, so only half of the domain is included in the simulation model to account for the bilateral symmetry of the setup.

The geometry of the floating platform is significantly simplified. Indeed, minor geometrical features that do not substantially influence the flow evolution were removed.

Three levels of refinement are used. Zone 1 defines a cube-shaped background mesh ($\Delta x_f = \Delta y_f = \Delta z_f$) with a cell size of 0.08 m; zone 2 is the first level of refinement with a cell size of 0.04 m, followed by zone 3, that uses a size of 0.01 m [15]. All the refinement regions extend stream-wise to the end of the domain. The dashed boxes in Fig. 2 show the customized Scotch decomposition domain. Due to current limitations in the parallelization algorithm, decomposed domains are adjusted to ensure that immersed boundaries do not span multiple processors.

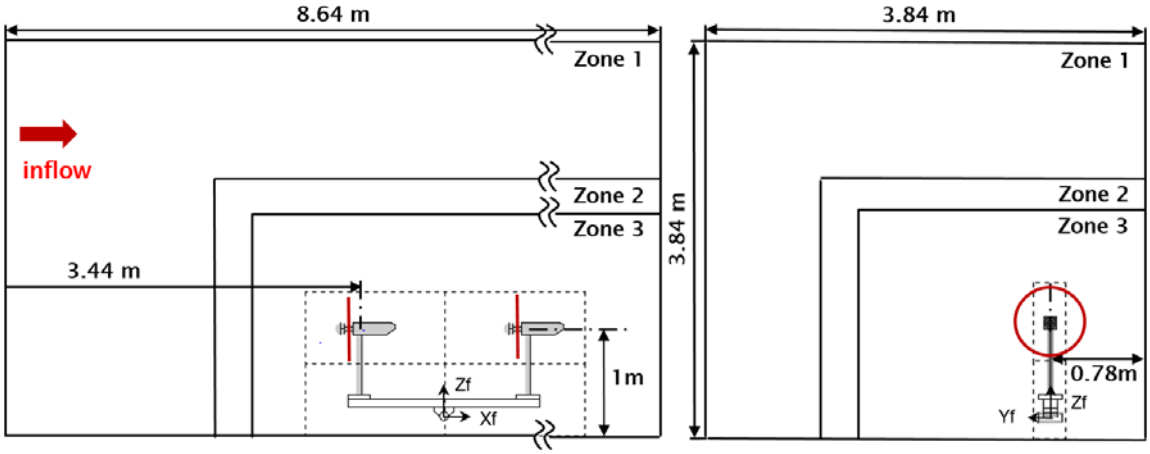

Figure 2: CFD computational domain. Left: lateral view; right: streamwise view.

Since the digital model tries to replicate the experiment, the simulation inflow speed, turbulence intensity and shear should be as close as possible to the experimental ones. In order to generate the proper inflow, a separate LES simulation is conducted that models the tunnel inlet, the spires and part of the wind tunnel chamber. A developed sheared and turbulent flow outflows from this sub-domain, which is then used as inflow for a second simulation, where the rest of the tunnel chamber and the wind turbines are modelled.

5. Results and analysis

Figure 3 shows instantaneous streamwise velocity and vorticity contours. The left part of the figure corresponds to a case where the platform is held fixed at null pitch. The two pictures on the right, on the other hand, correspond to the prescribed pitching case, the one in the center representing an instant in time when the platform is pitched forward, and the one on the right when the platform is pitched backward. The same sheared turbulent inflow is used for both the pitching and fixed platform simulations. A complex vertical wake meandering is observed in the pitching case (center and right), with a strong influence on the downstream machine and on the overall evolution of the combined wakes. Further analysis of the results is required to verify whether or not the pitching motion —and its induced wake meandering— influences or not wake recovery.

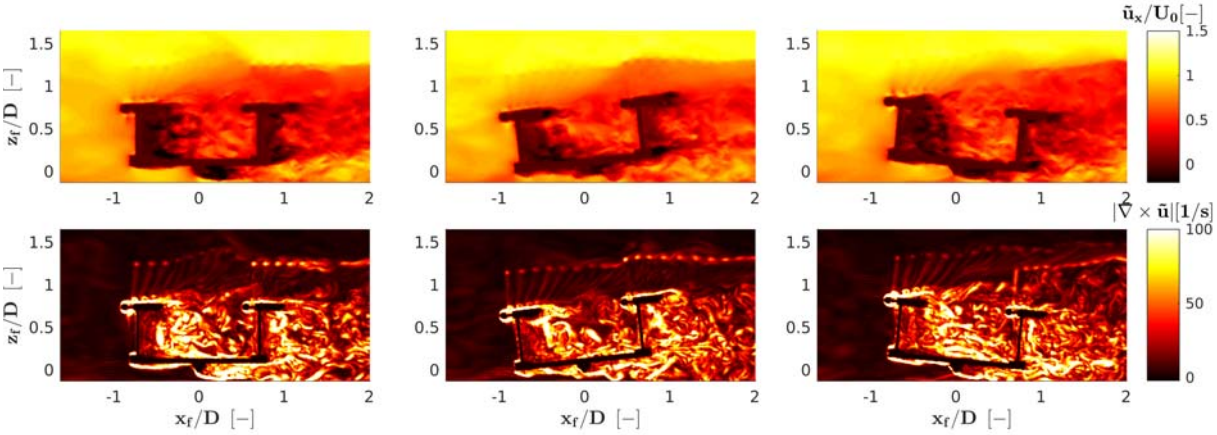

Figure 3: Normalized streamwise velocity (top) and vorticity (bottom) snapshots on the $x_f z_f$ plane through the turbine hubs. Left: fixed platform case; center and right: pitching case.

In the experiments, the bending moment at tower base is measured. Figure 4 depicts the system geometry, with the purpose of reconstructing the thrust T from the bending moment M_y, measured close to the tower base by strain gauges located at point o_s. Given the moving frame (x_s, z_s) attached to the tower, the equilibrium of moments around point o_s can be written as:

$$ma_{xf}Lcos(\theta - \beta_p) + m\dot{\Omega}L^2 + mgL(sin(\theta - \beta_p)) + ma_{zf}Lsin(\theta - \beta_p) = M_y + TH, \qquad (5)$$

where $a_{Os,xf}$ and $a_{Os,zf}$ are, respectively, the horizontal and vertical accelerations of point o_s, while $\dot{\Omega}$ is the angular acceleration of the platform, β_P the platform pitch angle, while the other geometrical quantities are defined in the figure. Since (x_s, z_s) is a non-inertial frame, one has to consider inertial forces applied at the center of mass o_m of the portion of wind turbine located above the load sensors. F_c is the centrifugal force, which however does not contribute to the moment equation since it passes through o_s; forces $ma_{Os,xf}$ and $ma_{Os,zf}$ are produced by the translational accelerations of o_s, while $m\dot{\Omega}L$ is due to the angular acceleration. Finally, m is the mass of the portion of wind turbine model located above the strain gauge. Coriolis forces are neglected, since only minor oscillations of the model center of gravity are expected due to tower vibrations.

Figure 5 shows the numerical and experimental time histories of the blade pitch angle β_B and rotor thrust T of the downstream machine, as well as the platform pitch angle β_P. While the pitch motion of the platform is fully known and exactly reproduced in the simulation, the turbulent wind can only be matched in a statistical sense. Therefore, one should not expect to

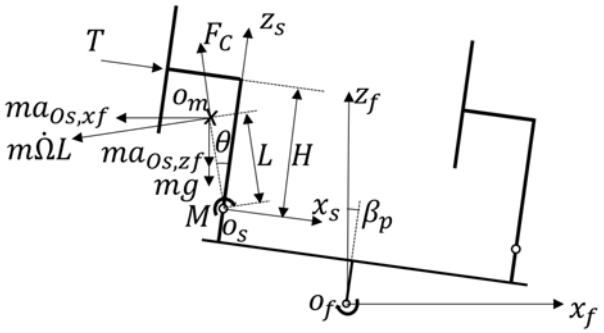

Figure 4: Sketch of the model geometry for the calculation of thrust from tower base bending moment.

observe an exact correspondence between simulation results and experimental measurements. A vertical wake meandering can clearly be observed both in the simulation and experimental results, as indicated by periodic oscillations of β_P and T for the downstream wind turbine. Such oscillation, however, are not observed for the upstream machine.

In both simulation and experiment, the wind turbines are governed by a collective pitch and toque controller. Since the machines operate in the full power regime, the goal of the controller is to keep the turbine power constant, compensating for the fluctuations due to pitching-induced wind changes and wind turbulence. Indeed, the power of the downstream machine in the simulation and experiment are both around the desired power output, i.e. 23.2 W. The blade pitch angle of the simulation shows a satisfactory accordance, in terms of magnitude and variation, with the one of the experiment. The periodic change of the blade pitch angle can be explained as follows: when the platform pitches nose down, i.e. the wind turbine is moving towards the incoming wind, the blade pitch angle increases to compensate for the increased relative inflow speed, and vice-versa. Similarly, the rotor thrust also changes periodically both in the simulation and the experiment.

Since the inflow conditions in the experiment and simulation only match in a statistical sense, the exact time histories of physical quantities can not be exactly reproduced in the simulation. Due to the relatively high computational cost of the CFD analysis, the current simulation only lasts for about 18 sec of physical time. For the results obtained so far, the mean thrust of the downstream wind turbine is equal to 9.6 N for the simulation and to 8.7 N for the experiment, while its standard deviation are 0.88 N and 1.05 N, respectively.

6. Conclusion and outlook

This paper has presented the application of a LES framework to a floating offshore multi-turbine platform. The developed approach is based on an existing LES solver, which was modified to handle a prescribed rigid body motion of the turbines. Rotor blades are modelled by lifting lines, while nacelle, tower and floating platform by an immersed boundary method. A complete restart capability allows to break long simulations into shorter consecutive segments. The wind turbines are operated in closed loop by a pitch and torque controller.

Data from a scaled FOWT experiment conducted in a boundary layer wind tunnel was used to verify the simulation model. The computational setup of the simulation strictly adheres to the experiment. A turbulent and sheared flow is passively generated in the experiment with spires placed at the tunnel inlet. The same process of turbulence generation was realized in the digital model, using an ad-hoc precursor simulation.

Results show that FOWT pitching introduces a vertical wake meandering, which affects the

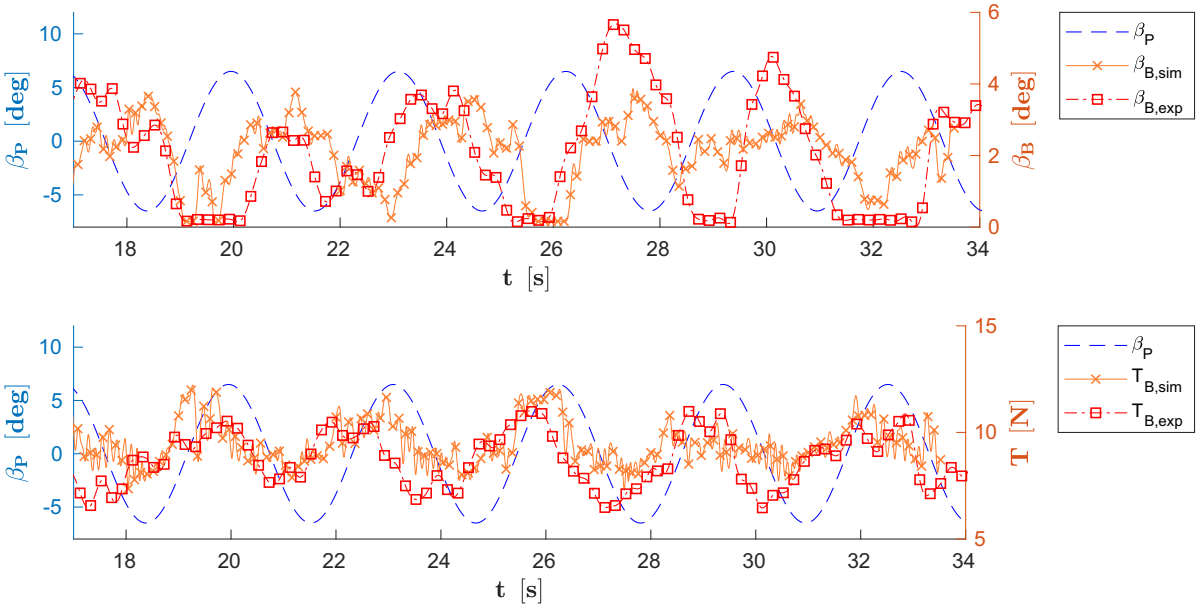

Figure 5: Comparison of numerical and experimental results for the downstream machine: blade pitch angle β_B (top) and rotor thrust T (bottom).

downstream machine. Both simulation and experimental results clearly indicate this effect, and show the compensation performed by the closed loop controller to keep a steady power output.

Given the small length of the numerical simulations performed so far, only a preliminary and rather qualitative comparison between simulation and experiment has been possible. Nonetheless, the simulation model seems to be capable of reproducing at least some of the characteristics of the response observed in the experiments.

In a continuation of this research activity, longer simulations will be conducted, which will enable a more accurate comparison of the results. The response of the machine in terms of mean and standard deviation of power, rotor speed, pitch and torque activity will be verified. In addition, the effect of platform pitching on wake recovery will be investigated. Different prescribed motions should be tested to better understand the resulting complex turbine to turbine interactions, as well as to back-scale the achieved results to a full-scale floating system.

7. Acknowledgements

The experimental work has been supported by the Korea Research Institute of Ships & Ocean Engineering (KRISO), through a contract with Technische Universität München. All tests were performed at the wind tunnel of the Politecnico di Milano, with the support of Prof. A. Croce, Mr. G. Campanardi and Mr. D. Grassi. The authors also express their appreciation to the Leibniz Supercomputing Centre (LRZ) for providing access and computing time on the SuperMUC Petascale System.

Nomenclature

CFD	Computational fluid dynamics
FOWT	Floating offshore wind turbine
LES	Large-eddy simulation

PISO	Pressure implicit with splitting of operator
TSR	Tip speed ratio
WT	Wind turbine
a_{xs}, a_{zs}	Acceleration components of point o_s
C_k	Corrected lift and drag coefficients
C_k^0	Nominal lift and drag coefficients
$\mathbf{f}_f$	Aerodynamic force in the fluid model reference frame
$\mathbf{f}_s$	Aerodynamic force in the structural model reference frame
F_c	Centrifugal force
H	Distance between hub and strain gauge
L	Length between center of mass and strain gauge o_s
m	Mass above the strain gauge
M_y	Tower base fore-aft bending moment
o_m	Center of mass
o_s	Origin of structural reference frame
o_s	Origin of fluid reference frame
$R(t)$	Time dependent direction cosine matrix
Re	Reynolds number
T	Rotor thrust
$\mathbf{x}_f$	Position in fluid model reference frame
$\mathbf{x}_s$	Position in structural model reference frame
(x_f, y_f, z_f)	Fluid domain coordinate frame
(x_s, y_s, z_s)	Structural domain coordinate frame
α	Angle of attack
β_B	Blade pitch angle
β_P	Platform pitch angle
Δ_k	Correction term of lift and drag coefficients
Δx_f, Δy_f, Δz_f	Cell size measured along the fluid coordinates
η	Non-dimensional blade span
θ	Angle between the tower axis and the line connecting o_m and o_s
φ	Platform angle between the tower axis and the line connecting o_s and o_f
ω	Angular velocity vector
$\dot{(\cdot)}$	Derivative with respect to time

References

[1] Bossanyi E 2000 The design of closed loop controllers for wind turbines *Wind Energy*, **3** 149-63
[2] Bottasso C L, Campagnolo F and Petrović V 2014 Wind tunnel testing of scaled wind turbine models: Beyond aerodynamics *Journal of wind engineering and industrial aerodynamics* **127** 11-18
[3] Campagnolo F, Petrović V, Bottasso C L and Croce A 2016 Wind tunnel testing of wake control strategies *Proceedings of the American Control Conference* 513-18
[4] Campagnolo F, Petrović V, Nanos E, Tan C, Bottasso C L, Paek I, Kim H and Kim K 2016 Wind tunnel testing of power maximization control strategies applied to a multi-turbine floating wind power platform *Proceedings of the International Offshore and Polar Engineering Conference* 309-16
[5] Campagnolo F, Croce A, Manos E, Petrović V, Schreiber J and Bottasso C L 2016 Wind tunnel testing of a closed-loop wake deflection controller for wind farm power maximization *Journal of Physics: Conference Series* **753**
[6] Campagnolo F, Petrovic V, Nanos E M, Tan C W, Bottasso C L, Paek I, Kim H and Kim K 2016 Wind tunnel testing of power maximization control strategies applied to a multi-turbine floating wind power platform *26th International Ocean and Polar Engineering Conference*
[7] Churchfield M and Lee S 2012 NWTC design codes-SOWFA. URL: http://wind. nrel. gov/designcodes/simulator s/SOWFA
[8] Jasak H, Weller H and Gosman A 1999 High resolution nvd differencing scheme for arbitrarily unstructured meshes *International journal for numerical methods in fluids* **31(2)** 431-49

[9] Jonkman J and Buhl M L 2004 *Fast user guide* (USA: Technical report, EL-500-29798, National Renewable Energy Laboratory, Golden, CO)
[10] Jasak H and Rigler D 2014 Finite volume immersed boundary method for turbulent flow simulations *9th OpenFOAM Workshop*
[11] Jonkman J and Buhl M L 2004 *Fast user guide* (USA: Technical report, EL-500-29798, National Renewable Energy Laboratory, Golden, CO)
[12] Kim K H, Lee K, Sohn J M, Park S W, Choi J S and Hong K 2015 Conceptual Design of 10MW Class Floating Wave-Offshore Wind Hybrid Power Generation System *25th International Ocean and Polar Engineering Conference*
[13] Kim H C, Kim M H, Kim K H, Hong K, Bae Y H 2016 Global Performance of a Square-Type Semi-Submersible KRISO Multi-Unit Floating Wind Turbine; Numerical Simulation vs Model Test *26th International Ocean and Polar Engineering Conference*
[14] Wang J, Foley S, Nanos E M, Yu T, Campagnolo F and Bottasso C L 2017 Numerical and experimental study for wake redirection techniques in a boundary layer wind tunnel *Journal of Physics: Conference Series* Wake Conference **854** 12-48
[15] Wang J, Liu Y, Campagnolo Fand and Bottasso C L 2018 Verification of a Fast Scale-Adaptive CFD Formulation for Waked Wind Turbines *2018 Wind Energy Symposium*, 02-51
[16] Wang J, Mclean D, Campagnolo F, Yu T and Bottasso C L 2017 Large-eddy simulation of waked turbines in a scaled wind farm facility *Journal of Physics: Conference Series* Wake Conference **854** 12-47
[17] Wang J, Chengyu W, Campagnolo F and Bottasso C L 2018 A large-eddy simulation approach for wind turbine wakes and its verification with wind tunnel measurements *Wind Energy Science* under review
[18] Zasso A, Giappino S, Muggiasca S and Rosa L 2005 Optimization of the boundary layer characteristics simulated at Politecnico di Milano Boundary Layer Wind Tunnel in a wide scale ratio range *Proceedings of the 6th Asia-Pacific Conference on Wind Engineering*